ChemPubSoc Europe
DOI: 10.1002/cphc.201500080
CHEMPHYSCHEM Minireviews

Mechanochemical Sensing: A Biomimetic Sensing Strategy

Prakash Shrestha, Shankar Mandal, and Hanbin Mao*[a]

Existing biosensors employ two major components: analyte recognition and signal transduction. Although specificity is achieved through analyte recognition, sensitivity is usually enhanced through a chemical amplification stage that couples the two main units in a sensor. Although highly sensitive, the extra chemical amplification stage complicates the sensing protocol. In addition, it separates the two elements spatiotemporally, reducing the real-time response of the biosensor. In this review, we discuss the new mechanochemical biosensors that employ mechanochemical coupling strategies to overcome these issues. By monitoring changes in the mechanical properties of a single-molecule template upon analyte binding, single-molecule sensitivity is reached. As chemical amplification becomes unnecessary in this single-molecule mechanochemical sensing (SMMS) strategy, real-time sensing is achieved.

1. Introduction

A biosensor contains two basic components: a biochemical recognition element and a physicochemical transducer.[1] The specific interaction between a sensing target (or analyte) and biorecognition element induces a physiochemical change in the transducer, which is translated into measurable chemical or physical output signals (e.g. luminescent, electrochemical, piezoelectric, or calorimetric signals, among others; see Figure 1). Commonly used recognition elements in biosensors include aptamers, antibodies/antigens, protein receptors/ligands, membranes, whole cells, and tissues.[1–2] To increase the detection limit, another element, chemical amplification, is often employed between the recognition and signal transduction components to generate strong signals for detection. An ideal biosensor should have high specificity in target recognition, low detection limit, ease of use, and excellent reproducibility. In the past few decades, biosensing devices that use optical[3] and electrochemical[4] signals have been developed with enhanced sensitivity, specificity, and usability.

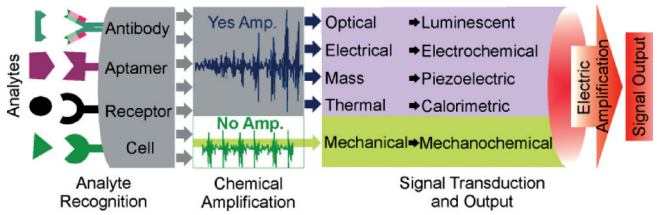

Figure 1. Schematic of a biosensor with commonly used biorecognition and signal transduction units. The mechanochemical sensing is depicted in the green channel at the bottom.

In particular, fluorescence-based biosensors with synthetic[5] or genetically encoded fluorophores[6] have revolutionized the development of bioanalyses in many fields. Either fluorescence intensity or wavelength can be used as a detecting signal.[6b] By using fluorescence imaging techniques, high-throughput screening of analytes can be achieved in different fields. However, special fluorophores used in a biosensor often require organic synthesis, increasing the cost of biosensing. In addition, bulky fluorophores should be carefully designed to avoid interference in the analyte recognition. Other disadvantages include prevalent background fluorescence noise, especially inside cells, as well as photobleaching of the dyes used in biosensors. Nanoscale electrochemical biosensors[7] can solve the problems associated with optical biosensors. As an electrochemical reaction is used in these biosensors, the photobleaching and background noise inherent in fluorescence-based sensing can be reduced. It also has unique advantages of simplicity in design, low cost, and portability.[8]

However, electrochemical biosensors require redox-active functional groups, which may, again, interfere with the recognition elements. In addition, the electrochemical biosensors developed so far measure average properties of analytes. Although ensemble-average approaches increase the reproducibility of sensing, they compromise the detection limit, as many molecules must be present to give recognizable signals with sufficient signal-to-noise ratios. The detection limit can often be improved by chemical amplifications through enzymatic approaches such as those used in the enzyme-linked immunosorbent assay (ELISA) and polymerase chain reaction (PCR), or with fuels used in various DNA-based biosensing strategies such as hybridization chain reaction (HCR),[9] rolling circle amplification (RCA),[10] and DNAzymes[11] (see Chemical Amplification in Figure 1). The employment of chemical amplification brings several unwarranted consequences. First, extra steps are involved in the biosensing. This complicates sensing protocols, increasing the cost and bringing extra noise associated with each additional step. Second, any amplification strategy re-

[a] P. Shrestha, S. Mandal, Prof. H. Mao
Department of Chemistry and Biochemistry
Kent State University, Kent, OH 44242 (USA)
E-mail: hmao@kent.edu

quires time to accomplish. This reduces the temporal resolution of the sensing, making real-time detection highly challenging. Finally, the amplification strategy is likely to be analyte dependent. This is especially problematic in PCR, as it is well known that the success of PCR is dependent on the sequence of DNA to be amplified.[12]

To eliminate these issues, it is desirable to develop amplification-free strategies. As amplification can no longer be considered, the detector for the sensor must be highly sensitive. Recently developed single-molecule techniques have made these types of detector readily available. With the capability of detecting single molecules, the ultimate detection limit in biosensing can be achieved. The most widely used method in single-molecule detection is fluorescence. However, owing to the photobleaching and extensive environmental background noise discussed above, fluorescence is not a reliable choice for single-molecule biosensing. An alternative approach is force-based single-molecule tools.[13] By attaching a single-molecule template, tension in a molecule can be controlled and monitored. If molecular tension can be correlated to analyte recognition, a new biosensing scheme can be generated.

Dr. Hanbin Mao obtained his PhD in Analytical Chemistry from Texas A&M University (USA) in 2003. He spent the next two years as Postdoctoral Associate at the University of California at Berkeley and the Lawrence Berkeley National Lab (USA). In 2005, he started his independent academic career at the Department of Chemistry and Biochemistry, Kent State University (USA). His main research interests are in the field of Mechanoanalytical Chemistry. His group has developed mechanochemical biosensors and investigated the structures and transition kinetics of biomacromolecules.

Prakash Shrestha received his B.Sc. in 2006 from Birendra Multiple Campus, Tribhuvan University (Nepal) and his M.Sc. in Chemistry from the same university in 2010. He was involved in teaching physical chemistry for 2 years before he joined the Department of Chemistry and Biochemistry, Kent State University (USA) in 2012. He is now working in Dr. Hanbin Mao's lab pursuing his doctoral degree. He is interested in the transition dynamics of nucleic acids and development of mechanochemical biosensors.

Shankar Mandal received his B.Sc. and M.S. in Chemistry from University of Dhaka (Bangladesh) in 2005 and 2007, respectively. He worked as a lecturer in the Department of Chemistry, University of Dhaka from 2010 to 2013. He is currently a PhD researcher in Dr. Hanbin Mao's research laboratory at the Kent State University (USA). His Ph.D research is focused on mechanochemical sensing at the single-molecule level.

2. Mechanochemical Coupling and Mechanochemistry

Mechanochemical coupling can serve as a missing link between chemical recognition and molecular tension in the sensing probe. In general, mechanochemical coupling describes the interaction between the mechanical property and the chemical property of a molecule. It is a subject of the newly emerged field, mechanochemistry. The term mechanochemistry can be traced back to the 1930s when Staudinger and coworkers reported that the reduction in molecular weight of polymers is subject to mastication,[14] which was later ascribed to the mechanical cleavage of covalent bonds in the polymers by Kauzmann and Erying.[15] The force-induced effects also change properties such as strength and elasticity of chain-like macromolecular polymers. Recently, the disassembly or change in mechanical properties of polymers has been attributed to functional groups known as mechanophores[14a,16] in the polymer under mechanical stress. In addition, changes in fluorescent properties of protein biocomposites caused by mechanical stress have been reported.[17]

Mechanical force is a universal variable that can be used to describe both microscopic and macroscopic processes such as electron–nucleus interactions, breaking or formation of chemical bonds, as well as various functions of tissues, organs, and engineering materials. Other than the covalent bonds in polymers, in which nanonewton forces are involved for the breaking of covalent bonds,[18] extensive efforts have been spent on investigating mechanochemical processes in noncovalent bonds. For example, piconewton forces have been shown to fold or unfold proteins, DNA, and RNA molecules.[13] In these investigations, the macromolecules are tethered by two polystyrene particles trapped in optical tweezers. The levitation of particles isolates the system from the environment, reducing the background noise. In addition, as no fluorophore is used, photobleaching is avoided in such a system. As a result, thousands of mechanical cycles can be performed in a span of days without compromising mechanical properties of a single-molecule template. All these properties forecast a potentially efficient single-molecule reporter that can be used in highly sensitive mechanochemical biosensors.

3. Mechanochemical Sensing

Many biological processes are associated with mechanochemical sensing, which is carried out by various cell compartments such as primary cilia or cell membranes by using mechanochemical coupling as the basic principle.[19] As a mechanochem-

ical sensor uses the same coupling mechanism, it is essentially a biomimetic device. So far, only a handful of mechanochemical sensing strategies have been reported,[20] most of which are cantilever based.[20c–h]

In 2000, Fritz and co-workers demonstrated mechanochemical sensing of biochemical reactions by using free-standing cantilevers.[20c] The authors used the change in the surface stress of cantilevers as a signal to follow DNA hybridization reactions. The sensitivity of the method allows differentiation of a single-base mismatch in two 12-mer oligonucleotides. In the following years, by monitoring changes in the micromechanical properties of the cantilevers, owing to various physical or chemical changes on their surfaces, different biochemical processes such as cell adhesion and protein recognition have been investigated.[20d–g]

By using a similar approach, the absorption of glucose molecules by living cells was determined by recording the change in the deflection pattern of the cantilever in an atomic force microscopy (AFM) instrument.[20h] In this method, Pei and coworkers immobilized glucose oxidase on the surface of an AFM cantilever. The presence of the glucose in a solution leads to the deflection of the cantilever, likely owing to the heat dissipated during the glucose-oxidase-catalyzed reaction on the cantilever surface. This was confirmed by inactive enzymes immobilized on the surface, which did not produce detectable deflections in the cantilever.

Although highly sensitive, these methods work in an ensemble-average manner. A silicon cantilever has dimensions ranging from sub-micrometers to micrometers, which contain zillions of silicon atoms. To induce a detectable change in the mechanical properties of this macroscopic subject, the number of interacting analytes should be on similar orders of magnitude. Even considering only the reactive surface of a cantilever 400×80 nm in size, it contains approximately 50 attomoles of silicon atoms with 0.111 nm as the Si radius.[21] To reach this scale, significant time should be spent to allow enough analyte molecules to interact with the cantilever. For analytes with low abundance, chemical amplification becomes necessary to complete the sensing in time. This, however, introduces extra noise and deteriorates the real-time response, as discussed above. In the case of the mechanochemical coupling through the reaction heat,[20h] substantial analytes should be turned over by an enzyme with a rate that surpasses the heat dissipation to the environment. The heat accumulation then changes the mechanical property of the cantilever. All these requirements complicate the sensing processes by compromising temporal resolution and narrowing the application scope. Therefore, it is desirable to reduce the scale of the sensing template. In the ultimate reduction, a single-molecule probe can be used for fast mechanical response upon interacting with only one analyte molecule. In the following sections of this Minireview, we will discuss single-molecule mechanochemical sensing (SMMS) methods that detect single analyte molecules through the direct measurement of a change in the tension or size in a single-molecule sensing template.

4. Single-Molecule Mechanochemical Sensing (SMMS)

As a sensing device, the ultimate detection limit in a biosensor is single analyte molecules. As the amount or size of detectable analytes scales with the mass or size of a sensing template, the smaller the template, the better the detection sensitivity. If a single-molecule template can be used, detection of individual analyte molecules becomes possible. In addition, the response of a single-molecule template can be rather fast. As soon as an analyte is bound to the probe, the response ensues as a result of single-molecule mechanochemical coupling. This is, in part, because the detection is so sensitive (i.e. single-molecule detection) that it is not necessary to wait for the binding of other analytes to achieve an effective detection.

Owing to the signal-to-noise issues discussed above, it is preferable to use force-based single-molecule tools instead of fluorescence-based approaches. The mechanical force, by virtue of its universal applicability, can be used to characterize almost all chemical interactions. The recognition component in biosensing is essentially a binding process between an analyte and the sensing template (Figure 1). As such, it can be characterized by the mechanical force. In SMMS, the same biochemical binding process is employed (Figure 2).

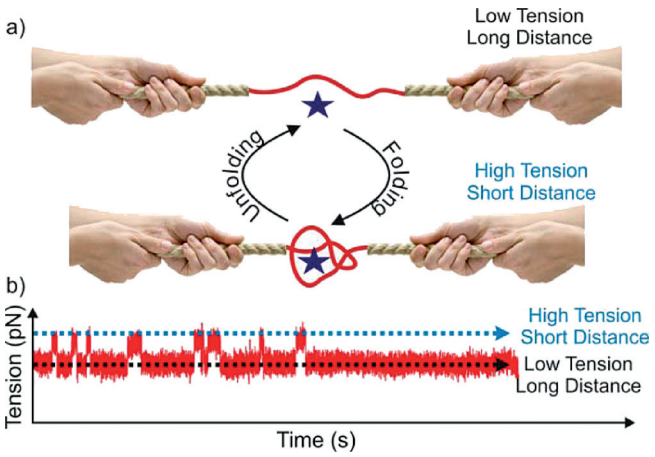

Figure 2. a) Schematic diagram depicting the reversible binding of an analyte molecule with a receptor in the single-molecule template. The binding induces folding of a structure, which reduces the length of the template with increased tension in the template. b) A time-lapse trace depicting the reversible binding event.

The reversible binding process is traditionally described by a thermodynamic dissociation constant, K_d. As it is a thermodynamic parameter, it does not give detailed kinetic information, which is important for a sensing process. Recently, the concept of mechanical affinity was proposed to account for the kinetics in the binding process.[22] Mechanical affinity of a ligand–receptor complex is defined as the amount of work to dissociate a ligand–receptor complex ($W_{affinity}$), which is equivalent to the difference between the work of dissociating a receptor–ligand complex by unfolding the bound receptor ($W_{complex\text{-}unfold}$) and that to unfold the free receptor ($W_{receptor\text{-}unfold}$) [Eq (1)]:

$$W_{affinity} = W_{complex\text{-}unfold} - W_{receptor\text{-}unfold} \quad (1)$$

As the unfolding work describes a kinetic process that is dependent on a specific reaction path, the mechanical affinity reflects the kinetics of the binding between a ligand and a receptor. The kinetic nature of the unfolding work can be understood by the relative movement between the ligand and receptor during the disassembly. Such a motion causes dissipation of friction heat, which must be covered by the work needed to disassemble the pair. Depending on the unfolding angles, the relative motion between the ligand and the receptor varies, leading to different frictions. As a result, the work of unfolding and the mechanical affinity is anisotropic. The anisotropic property has been experimentally verified in single-molecular force spectroscopy experiments.[23] In theory, any of the unfolding directions can be used to monitor analyte binding in SMMS, which renders the versatility of the method. In practice, the direction with the biggest change in the mechanical property is often selected. By repeatedly collecting many mechanical affinity ($W_{affinity}$) values along a particular direction, the chemical affinity ($\Delta G_{affinity}$) can be retrieved by using Jarzynski's nonequilibrium theorem [Eq. (2)]:[24]

$$\Delta G_{affinity} = -k_B T \ln \sum_{i=1}^{N} \frac{1}{N} \exp\left(-\frac{W_{affinity,i}}{k_B T}\right) \quad (2)$$

where N is the total number of measurements, k_B is the Boltzmann constant, and T is absolute temperature.

After biochemical recognition through ligand–receptor binding on a single-molecule template, signal transduction is carried out in the second component of the SMMS. Compared to regular biosensing, which often employs chemical amplification to increase the intensity of a signal, in SMMS, the chemical amplification is not necessary given the single-molecule detection capability of the detector. In force-based single-molecule techniques, the change in the tension or extension of the probe is monitored through the mechanochemical coupling. Such a coupling converts the chemical recognition events to the mechanical (force or space) response (Figure 2). For example, the sensing template can be maintained at a constant tension to populate a macromolecule in an unfolded state. Binding of the analyte induces the folding of the macromolecule, shortening the extension of the sensing template given the constant tension. If, however, the extension of the template is maintained as constant, the folded macromolecule then increases the tension in the probe. Either the change in the extension or the tension can be monitored in an instrument for force manipulation.

4.1. Instruments used for SMMS

Rapid advancement in force-based single-molecule instrumentation in biophysics and related fields has offered a variety of choices that can be employed in the SMMS.

AFM was developed[25] on the basis of the scanning tunneling microscopy (STM).[26] After decades of development, AFM has become one of the most widely used tools for high-resolution imaging and mechanochemical manipulation of nucleic acids or proteins in the range of pico- to nanonewtons. A microfabricated cantilever with a highly delicate tip (in atomic scale) is used as a probe in AFM. There are various types and modes of AFM for particular applications. For single-molecule force manipulation, a molecule is first tethered between the cantilever tip and the surface of a substrate (Figure 3a). When the substrate surface that is controlled by a piezoelectric device is moved, the tension in the molecule changes, which can be measured by the deflection of the cantilever. Advanced AFM instruments have spatial resolution on a nanometer scale and force resolution on a piconewton scale. Such spatial and force resolutions are sufficient to follow biochemical binding at the single-molecular level.

Magnetic tweezers represent a more recently developed single-molecule tool. In this method, a molecule of interest is tethered between a magnetically trapped microparticle and the surface of a substrate (Figure 3b). This instrument permits a unique feature to investigate the effect of torque on a molecule by rotating the magnetic particle. The force resolution of magnetic tweezers goes down to sub-piconewton level, which is better than other methods. However, in many cases, the measurement of force is based on diffraction patterns with involved calculations.

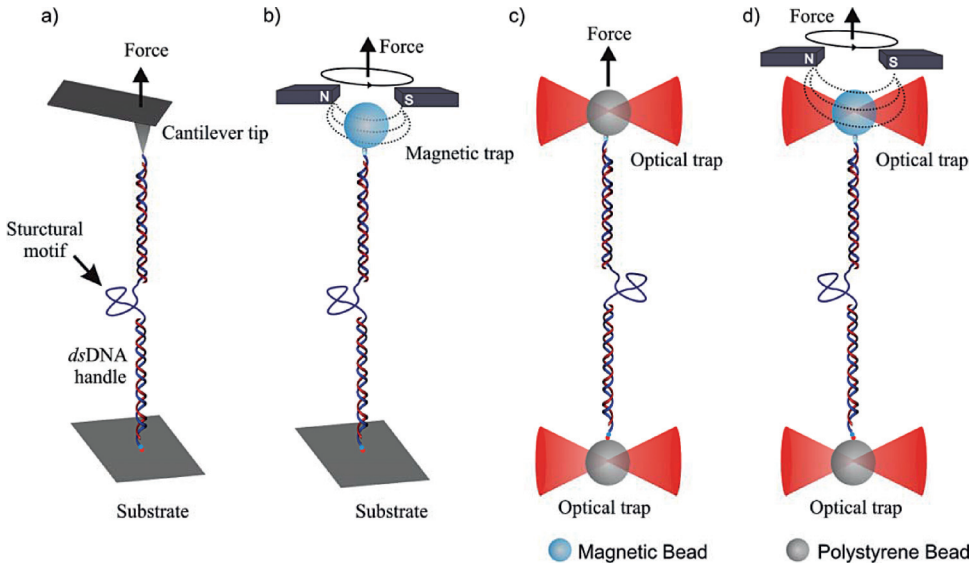

Figure 3. Setups for single-molecule force manipulations. a) AFM, b) magnetic tweezers, c) optical tweezers, and d) magneto-optical tweezers. A DNA molecule that contains a receptor is shown as an example between two surfaces.

Ashkin and co-workers developed optical tweezers in 1986.[27] The instrument has since been widely adopted in single-molecule biophysics.[28] In this method, laser beams are exploited to trap dielectric microparticles. Single-beam and dual-beam laser trappings represent the two main types of the instrument. In single-beam optical tweezers, a laser-trapped dielectric particle is used to grab one end of a molecule. The other end of the molecule is attached to a solid surface either covalently or through a bead immobilized at the tip of a pipette through suction.[29] In dual-beam optical tweezers,[30] the molecule is tethered between two optically trapped beads by using affinity linkages (Figure 3c). As both beads are levitated away from any surface, the differential drift associated with the solid surface and the laser foci is eliminated, reducing the mechanical noise. The dual-beam laser-trap instruments have a better force resolution (10^{-13}–10^{-10} N) than AFM (10^{-11}–10^{-7} N). Moreover, the sub-nanometer spatial resolution allows investigation of interactions between proteins and nucleic acids at the single base-pair level.[31]

Recently, Selvam and co-workers designed a new instrument, magneto-optical tweezers.[32] In this method, a magnetic bead and a polystyrene bead are trapped in two optical traps and a molecule of interest is tethered between these two beads through affinity linkages (Figure 3d). A pair of magnets on top of the magnetic bead is used to rotate the magnetic bead to introduce torque in a molecule whose ends are tethered to surfaces with a torsionally constrained manner. The magneto-optical tweezers combine the advantages of easy manipulation of a magnetic-tweezers instrument in torque generation and high resolution of dual-trap optical tweezers.

4.2. Templates used in SMMS

Due to the superior spatial and force resolutions, as well as high mechanical stability, dual-beam laser tweezers are used in SMMS. In most cases, a DNA template is used as a sensing template, owing to its easy synthesis and high stability. In force-based single-molecule biophysical investigations, duplex DNA strands have been used extensively as handles to tether biomacromolecules of interest. It has been well recognized that most plasmid or Lambda dsDNA strands have few secondary structures, which can interfere with the signal interpretation in SMMS. Recent developments in DNA nanotechnology such as DNA aptamers and DNA origami's[33] have provided a rich repertoire to construct DNA-based receptors for the recognition of a variety of analytes. In addition to this prior knowledge, a myriad of molecular biology techniques, such as PCR and splint ligation,[34] are available to incorporate DNA-based receptors into the dsDNA handles. During the construction of a sensing template, a DNA probe is first inserted between two dsDNA handles by using molecular biology methods. The DNA construct is then tethered between two optically trapped particles in a dual-beam laser tweezers instrument to monitor the change in force or extension upon binding of an analyte to the single-molecule probe. The first-in-class SMMS device was demonstrated by Koirala and co-workers for the detection of single nucleotide polymorphism (SNP) by using a DNA hairpin as a probe.[35] In a recent development, novel strategies have been developed to increase the throughput and render multiplexing capability of the sensing by exploiting DNA nanoassemblies.[36]

4.2.1. *One-Dimensional Templates*

Single-stranded DNA oligomers or DNA aptamers that can recognize a complementary sequence or specific small molecule ligands, respectively, are defined as one-dimensional (1D) templates. A few SMMS examples have been reported for the detection of DNA and small molecules.

4.2.1.1. SNP Detection in SMMS

Owing to its close association with the susceptibility and diagnosis of diseases,[37] SNP is of high interest in biosensing. In the SMMS sensor demonstrated by Koirala and co-workers (Figure 4),[35] a DNA hairpin was used as a SNP probe. The loop and a section of the hairpin stem were designed to recognize DNA targets by using Watson–Crick base pairing. Owing to increased thermodynamic stability, the binding of DNA targets to the hairpin is expected to unfold the hairpin, causing

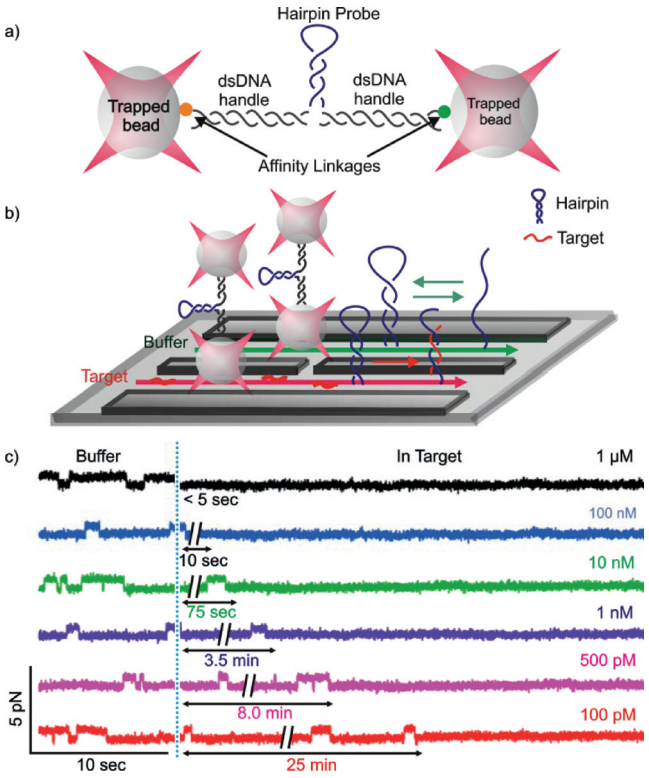

Figure 4. Schematic of a SMMS strategy to detect SNP by using a DNA hairpin probe. a) A hairpin containing a SNP probe that recognizes a specific SNP target is sandwiched between two dsDNA handles, which are tethered to two optically trapped beads. b) Sensing mechanism for the SNP probe in a microfluidic device. c) Hopping traces for the SNP probe with different target concentrations. The vertical dotted line indicates the transfer of the SNP probe from the buffer to the target channel. Double-headed arrows depict the average time observed before the hopping ceases to the unfolded hairpin state, which indicates the binding of the SNP to the hairpin.

a change in the tension or extension of the sensing probe (Figures 4a and b). Before the SMMS experiment, the probe was sandwiched between the two dsDNA handles, which were anchored to two optically trapped beads. To perform real-time SNP detection, a microfluidic chamber with interconnected channels was used (Figure 4b). Such a design allows the flow of desired buffers in different channels while ensuring free movement of the SNP probe between the channels. During the sensing, by maintaining a constant extension of the DNA construct, the DNA hairpin inside the construct undergoes transitions rapidly between the folded and unfolded states (bi-state hopping) in the buffer channel. As soon as the hairpin probe was moved to the channel that contains the SNP target, the binding of the SNP to the hairpin unfolded the hairpin, ceasing bi-state hopping (Figure 4c). Within 30 min, this SMMS strategy can detect as low as 100 pM of an SNP target associated with coronary diseases without using any amplification steps. The detection limit can be further improved by optimizing the flow rate and reducing the channel cross-section, for example.[35] Owing to the one-dimensional sensing probe used in this sensing strategy, the throughput of this method is limited.

4.2.1.2. Small-Molecule Sensing

By using DNA aptamers as a probe, small molecules can be recognized in the one-dimensional DNA template (Figure 5).[38] With this SMMS strategy, the binding constant (K_d) between an aptamer and a small molecule, ATP, was successfully measured in optical tweezers.[38] The K_d was estimated from a change in the free energy of the binding between the ATP and the aptamers ($\Delta G_{binding}$) by using the relationship $\Delta G_{binding} = -RT\ln K_d$,

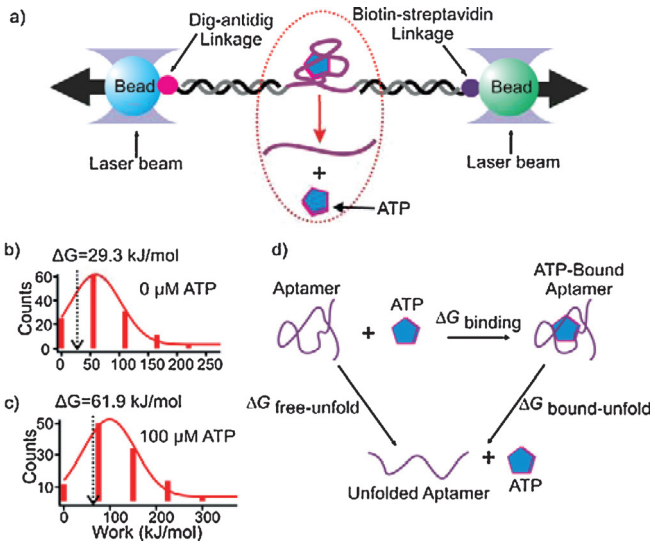

Figure 5. a) Experimental setup to detect the binding interaction of the small molecule ATP with an aptamer, which is sandwiched between two optically trapped beads through two dsDNA handles. Histograms of the work done to unfold b) the free aptamer and c) ATP-bound aptamer. Dotted arrows show the work equivalent to the change in free energy of unfolding (ΔG_{unfold}). d) Hess-like cycle of the aptamer–ATP binding process used for the calculation of the $\Delta G_{binding}$ and the determination of K_d.

where R is the gas constant and T is temperature. As the change in free energy is a state function, a Hess-like cycle was used to retrieve the $\Delta G_{binding}$ value (Figure 5d). For this purpose, the change in the free energy of unfolding the free aptamer ($\Delta G_{free\text{-}unfold}$) and that of bound aptamers ($\Delta G_{bound\text{-}unfold}$) were first converted from respective unfolding works by using Jarzynski's nonequilibrium theorem.[39] The difference between these two ΔG values then gives $\Delta G_{binding}$. The dissociation constant (K_d) was thus estimated as 2.0 ± 0.2 μM, which is consistent with the literature.[40] It is noteworthy that this technique offers a unique advantage to determine K_d for aptamer–ligand interactions by using only one ligand concentration.[41] In comparison, many conventional techniques, such as fluorescence-based assays, require a series of experiments with varying ligand or aptamer concentrations to obtain K_d.

Similar experiments were performed for the recognition of a ligand, pyridostatin (PDS), to the telomeric G-quadruplex,[42] which is suggested to play a role in maintaining the length of telomere, a hallmark for the cancer genesis.[43]

4.2.2. Two-Dimensional SMMS Templates

The limited dimension in the 1D DNA templates leads to low throughput and lack of multiplex sensing. These problems can be addressed by expanding the dimensions of the SMMS templates. Recent rapid progress in DNA nanotechnology[33b,36,44] has made this task within reach. For example, by using the flexible synthetic strategy of DNA origami nanostructures, multiple DNA aptamer probes can be incorporated. As a proof of concept demonstrated recently, a seven-tile 2D DNA origami template was synthesized, which was then tethered between two optically trapped beads through two dsDNA handles using affinity linkages (Figure 6a). The seven origami tiles were connected in such a way that adjacent DNA tiles were locked by the hybridization of two complementary DNA strands attached to the two respective tiles. One of the locking DNA strands contained an aptamer that can recognize the target (platelet-derived growth factor, or PDGF). During the sensing, binding of the target to the DNA aptamer compromised the Watson–Crick base pairing in the two DNA locking strands, which unlocked adjacent tiles (Figure 6b). The successful synthesis of this origami construct was characterized by using AFM as well as force ramping experiments in optical tweezers. Typical force–extension (F-X) curves showed more than six force-induced unlocking events, as expected when no target molecules were present (shown by arrowheads in Figure 6c). Upon incubation with PDGF (50 nM) prior to the force ramping experiment, no unlocking events were observed in F-X curves in the SMMS template, indicating that the binding of PDGF had already unlocked the tiles (Figure 6c, red trace).

After successful characterization of the single-molecule DNA origami construct, a constant force (8 pN) was maintained in the SMMS template with and without PDGF for real-time biosensing. No recognition events were observed in the absence of PDGF, whereas sudden changes in extension occurred after switching to the target solution (25 nM PDGF) (pointed by arrowheads in Figure 6d). The detection limit was estimated to

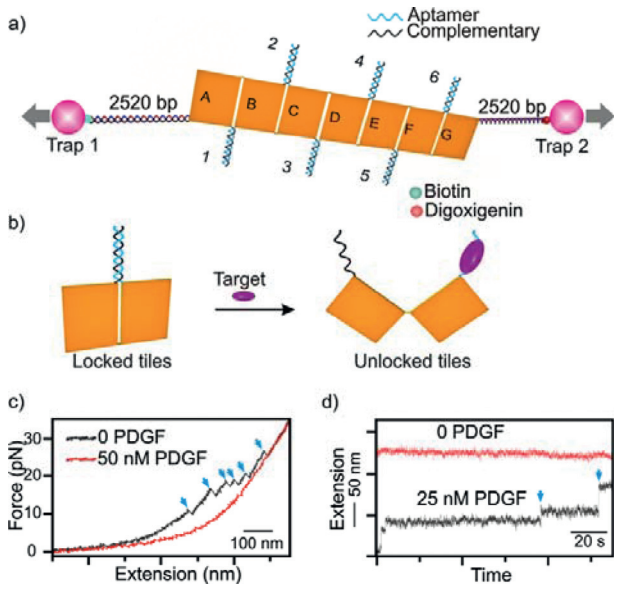

Figure 6. Mechanochemical biosensing using DNA origami nanostructures with increased throughput in optical tweezers. a) Schematic of a seven-tile 2D DNA origami nanoassembly tethered between two optically trapped beads through two dsDNA handles modified with terminal digoxigenin and biotin. The adjacent tiles are locked by aptamer DNA (blue) and its complementary strand (black) (marked 1–6). b) Illustration of the tile unlocking because of the target binding to an aptamer lock. c) Representative F-X curves of the seven-tile DNA nanoassembly in the absence (gray) and presence (red) of 50 nM PDGF. The force-induced unlocking events (arrowheads) were absent in the solution containing the PDGF. d) Real-time observation of the target recognition events when a constant force (8 pN) was maintained in the probe. Without PDGF, no recognition events were observed. When the probe was switched to the PDGF solution, the binding of the target unlocked the tiles, leading to the extension jumps (arrowheads).

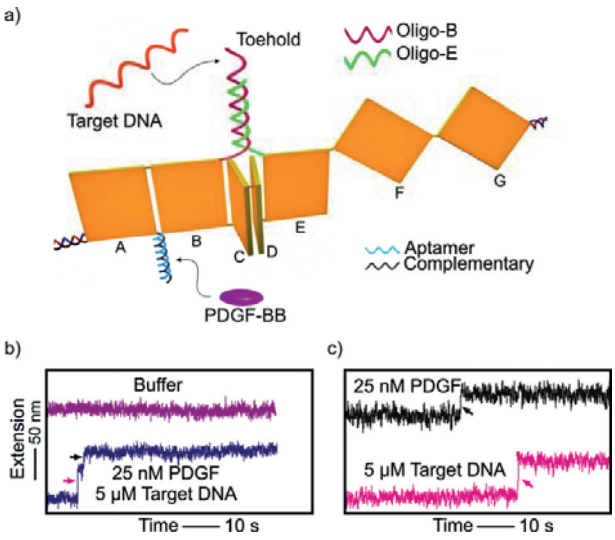

Figure 7. a) Schematic of the sensing platform when using a 3D origami nanoassembly. The lock between tiles A and B contains a PDGF aptamer, whereas that between the tiles B and E consists of a toehold DNA strand. All other tiles remain unlocked. b,c) Real-time detection of multiple targets when a constant force of 8 pN was maintained in the probe. In target free solution (b), the sensor showed no extension jumps. When both targets were present, two extension-jumps corresponding to the breaking of the two locks were observed. However, in the solution that contains only one target (c), one extension jump was observed.

be 10 pM (3σ) within 10 min for the binding of PDGF to at least one probe. Compared to the 100 pM detection limit in 30 min in the 1D DNA template discussed above, this detection limit clearly shows that multiple-aptamer probes can improve the sensitivity while significantly reducing the detection time.

4.2.3. Three-Dimensional SMMS Templates

To further improve the throughput, it is desirable to use a template with a more compact design. A 3D template offers such an opportunity, as the space can be utilized more efficiently. To demonstrate this, a 3D DNA origami nanostructure comprising multiple recognition elements was synthesized.[36] This design was based on a previously used seven-tile origami nanoassembly (Figure 7a). Tiles A and B were locked by the same aptamer-containing complementary DNA strands, as discussed previously for the PDGF recognition. Tiles B and E were interconnected by two other complementary DNA strands, in which the DNA strand from tile B contained a toehold region to facilitate the recognition of a DNA target with complementary sequence. Typical F-X curves showed two unlocking events in the target-free solution, which corresponded to the force-induced unlocking of the tiles between A–B and B–E, respectively. In the presence of one of the targets, one unlocking event corresponding to a specific target was observed. No unlocking events were observed in the presence of both targets (50 nm PDGF and 5 μm target DNA), indicating prior disassembly of the locks upon target binding.

Next, a constant tension (8 pN) was maintained inside the DNA construct for real-time detection of multiple targets. The sensor showed no change in extension in the target-free solution (Figure 7b, pink trace), whereas two extension jumps, corresponding to the unlockings of the two locks, were observed when both targets (Figure 7b, blue trace) were present. As expected, only one extension change was observed in the presence of one target in the buffer (Figure 7c). Owing to different locking arrangements in the 3D template, this method can easily recognize specific targets through the change in extension accompanied with the target binding. Although the lock between tiles A and B brings an extension change of approximately 15 nm, the lock between tiles B and E gives much larger extension change of approximately 40 nm. Taking advantage of copious 3D spatial arrangements, as demonstrated in many origami DNA nanostructures, the multiplexing capability can be well achieved for more targets.

5. Conclusions and Prospects

In this work, a new biosensing strategy, mechanochemical sensing, has been reviewed. In this sensing method, mechanochemical coupling is exploited to convert chemical recognition to mechanical signals, which are represented by tension or extension of a probing template. It is, thus, fundamentally different from current biosensors, in which spatiotemporally separated analyte recognition and signal transduction units are

coupled by time-consuming chemical amplification modules. A fast response is achieved for mechanochemical coupling, especially at the single-molecule level. This not only allows real-time detection of analyte molecules, the streamlined design also reduces extra noise imparted by additional coupling elements. The single-molecule template offers the capability to detect individual analyte molecules, which represents the Holy Grail in the mass-detection limit of biosensing. By incorporating a DNA-based recognition element in single-molecule DNA templates, the SMMS strategy fully exploits the knowledge and techniques blossomed in rapidly developing fields such as DNA nanotechnology, molecular biology, as well as non-B DNA structures such as hairpins, G-quadruplexes, and i-motifs.[45] The generic nature and high sensitivity of SMMS have been reflected in the facile detection of picomolar amounts of small molecules, nucleic acids, as well as macromolecular biomolecules, such as peptides, on a microfluidic platform within 30 min. By optimizing the microfluidic design and extending the time window for detection, this detection limit can be readily improved.

Although 3D DNA nanostructures can be employed to improve the throughput and multiplexing capabilities in SMMS, the cost and the complexity of DNA nanoassembly become a concern. Future development of SMMS should aim to solve this problem. Instead of using DNA nanostructures as sensing templates, one possible alternative is to use cheaper and more robust inorganic nanostructures such as 2D graphene sheets as carriers for sensing probes.

With a broader perspective, mechanochemical sensing is a subject in the framework of mechanoanalytical chemistry, which uses mechanical means to analyze chemical problems.[36,46] As discussed above, mechanical force is a universal variable to describe a range of systems, including those in chemistry. However, limited by the available tools, such a description has just started to take place in chemistry. The toolkit of mechanochemical sensing is one example to fill the gap of our understanding on the fundamental aspects of mechanical variables on chemical systems.

Acknowledgements

This work was supported by the National Science Foundation through NSF CHE-1026532 and NSF CHE-1415883.

Keywords: biosensors · DNA · mechanochemical sensing · optical tweezers · single-molecule techniques

[1] a) D. R. Thévenot, K. Toth, R. A. Durst, G. S. Wilson, *Biosens. Bioelectron.* **2001**, *16*, 121 – 131; b) T. Anthony, W. George, K. Isao, *Biosensors: Fundamentals and Applications*, Oxford University Press, Oxford, **1987**.

[2] K. Cammann, *Fresenius Z. Anal. Chem.* **1977**, *287*, 1 – 9.

[3] S. F. Pennathur, D. K. Fygenson, *Lab Chip* **2008**, *8*, 649 – 652.

[4] N. Wongkaew, P. He, V. Kurth, W. Surareungchai, A. Baeumner, *Anal. Bioanal. Chem.* **2013**, *405*, 5965 – 5974.

[5] a) X. Tan, Y. Wang, B. A. Armitage, M. P. Bruchez, *Anal. Chem.* **2014**, *86*, 10864 – 10869; b) M. A. Brun, R. Griss, L. Reymond, K.-T. Tan, J. Piguet, R. J. R. W. Peters, H. Vogel, K. Johnsson, *J. Am. Chem. Soc.* **2011**, *133*, 16235 – 16242; c) M. A. Brun, K.-T. Tan, R. Griss, A. Kielkowska, L. Reymond, K. Johnsson, *J. Am. Chem. Soc.* **2012**, *134*, 7676 – 7678; d) S. Tyagi, F. R. Kramer, *Nat. Biotechnol.* **1996**, *14*, 303 – 308.

[6] a) K. Tainaka, R. Sakaguchi, H. Hayashi, S. Nakano, F. F. Liew, T. Morii, *Sensors* **2010**, *10*, 1355 – 1376; b) S. Okumoto, A. Jones, W. B. Frommer, *Annu. Rev. Plant Biol.* **2012**, *63*, 663 – 706; c) M. C. Morris, *Biochim. Biophys. Acta* **2013**, *7*, 1; d) H. Wang, E. Nakata, I. Hamachi, *ChemBioChem* **2009**, *10*, 2560 – 2577; e) T. Ozawa, H. Yoshimura, S. B. Kim, *Anal. Chem.* **2013**, *85*, 590 – 609; f) W. B. Frommer, M. W. Davidson, R. E. Campbell, *Chem. Soc. Rev.* **2009**, *38*, 2833 – 2841.

[7] a) H. Bayley, P. S. Cremer, *Nature* **2001**, *413*, 226 – 230; b) B. L. Allen, P. D. Kichambare, A. Star, *Adv. Mater.* **2007**, *19*, 1439 – 1451; c) G. Gruner, *Anal. Bioanal. Chem.* **2006**, *384*, 322 – 335; d) S. Liu, Q. Shen, Y. Cao, L. Gan, Z. Wang, M. L. Steigerwald, X. Guo, *Coord. Chem. Rev.* **2010**, *254*, 1101 – 1116.

[8] X. Guo, *Adv. Mater.* **2013**, *25*, 3397 – 3408.

[9] a) D. Y. Zhang, G. Seelig, *Nat. Chem.* **2011**, *3*, 103 – 113; b) R. M. Dirks, N. A. Pierce, *Proc. Natl. Acad. Sci. USA* **2004**, *101*, 15275 – 15278.

[10] B. Schweitzer, S. Wiltshire, J. Lambert, S. O'Malley, K. Kukanskis, Z. Zhu, S. F. Kingsmore, P. M. Lizardi, D. C. Ward, *Proc. Natl. Acad. Sci. USA* **2000**, *97*, 10113 – 10119.

[11] R. R. Breaker, G. F. Joyce, *Chem. Biol.* **1994**, *1*, 223 – 229.

[12] a) J. S. Bartlett, D. Stirling, in *PCR Protocols, Vol. 226* (Eds.: J. S. Bartlett, D. Stirling), Humana Press, **2003**, pp. 3 – 6; b) R. K. Saiki, D. H. Gelfand, S. Stoffel, S. J. Scharf, R. Higuchi, G. T. Horn, K. B. Mullis, H. A. Erlich, *Science* **1988**, *239*, 487 – 491.

[13] a) J. Liphardt, B. Onoa, S. B. Smith, I. Tinoco, Jr., C. Bustamante, *Science* **2001**, *292*, 733 – 737; b) M. T. Woodside, W. M. Behnke-Parks, K. Larizadeh, K. Travers, D. Herschlag, S. M. Block, *Proc. Natl. Acad. Sci. USA* **2006**, *103*, 6190 – 6195.

[14] a) P. A. May, J. S. Moore, *Chem. Soc. Rev.* **2013**, *42*, 7497 – 7506; b) H. Staudinger, H. F. Bondy, *Ber. Dtsch. Chem. Ges.* **1930**, *63*, 734 – 736.

[15] W. Kauzmann, H. Eyring, *J. Am. Chem. Soc.* **1940**, *62*, 3113 – 3125.

[16] a) M. M. Caruso, D. A. Davis, Q. Shen, S. A. Odom, N. R. Sottos, S. R. White, J. S. Moore, *Chem. Rev.* **2009**, *109*, 5755 – 5798; b) Z. S. Kean, S. L. Craig, *Polymer* **2012**, *53*, 1035 – 1048; c) J. N. Brantley, K. M. Wiggins, C. W. Bielawski, *Polym. Int.* **2013**, *62*, 2 – 12.

[17] J. N. Brantley, C. B. Bailey, J. R. Cannon, K. A. Clark, D. A. Vanden Bout, J. S. Brodbelt, A. T. Keatinge-Clay, C. W. Bielawski, *Angew. Chem. Int. Ed.* **2014**, *53*, 5088 – 5092; *Angew. Chem.* **2014**, *126*, 5188 – 5192.

[18] M. Grandbois, M. Beyer, M. Rief, H. Clausen-Schaumann, H. E. Gaub, *Science* **1999**, *283*, 1727 – 1730.

[19] a) H. Muhammad, Y. Rais, N. Miosge, E. Ornan, *Cell. Mol. Life Sci.* **2012**, *69*, 2101 – 2107; b) I. Rayment, H. M. Holden, M. Whittaker, C. B. Yohn, M. Lorenz, K. C. Holmes, M. R. Milligan, *Science* **1993**, *261*, 58 – 65; c) K. Visscher, M. J. Schnitzer, S. M. Block, *Biophys. J.* **1999**, *76*, A43 – A43.

[20] a) Y. Liu, K. Yehl, Y. Narui, K. Salaita, *J. Am. Chem. Soc.* **2013**, *135*, 5320 – 5323; b) B. L. Blakely, C. E. Dumelin, B. Trappmann, L. M. McGregor, C. K. Choi, P. C. Anthony, V. K. Duesterberg, B. M. Baker, S. M. Block, D. R. Liu, C. S. Chen, *Nat. Methods* **2014**, *11*, 1229 – 1232; c) J. Fritz, M. K. Baller, H. P. Lang, H. Rothuizen, P. Vettiger, E. Meyer, H.-J. Güntherodt, C. Gerber, J. K. Gimzewski, *Science* **2000**, *288*, 316 – 318; d) J. Park, J. Ryu, S. K. Choi, E. Seo, J. M. Cha, S. Ryu, J. Kim, B. Kim, S. H. Lee, *Anal. Chem.* **2005**, *77*, 6571 – 6580; e) N. Backmann, C. Zahnd, F. Huber, A. Bietsch, A. Plückthun, H.-P. Lang, H.-J. Güntherodt, M. Hegner, C. Gerber, *Proc. Natl. Acad. Sci. USA* **2005**, *102*, 14587 – 14592; f) M. Watari, J. Galbraith, H.-P. Lang, M. Sousa, M. Hegner, C. Gerber, M. A. Horton, R. A. McKendry, *J. Am. Chem. Soc.* **2007**, *129*, 601 – 609; g) R. McKendry, J. Zhang, Y. Arntz, T. Strunz, M. Hegner, H. P. Lang, M. K. Baller, U. Certa, E. Meyer, H.-J. Güntherodt, C. Gerber, *Proc. Natl. Acad. Sci. USA* **2002**, *99*, 9783 – 9788; h) J. Pei, F. Tian, T. Thundat, *Anal. Chem.* **2004**, *76*, 292 – 297.

[21] K. W. Whitten, R. E. Davis, M. L. Peck, G. G. Stanley, *Chemistry*, 9th ed., Mary Finch, Belmont, **2010**.

[22] D. Koirala, P. M. Yangyuoru, H. Mao, *Rev. Anal. Chem.* **2013**, *32*, 197 – 208.

[23] a) H. Clausen-Schaumann, M. Seitz, R. Krautbauer, H. E. Gaub, *Curr. Opin. Chem. Biol.* **2000**, *4*, 524 – 530; b) Z. Yu, D. Koirala, Y. Cui, L. F. Easterling, Y. Zhao, H. Mao, *J. Am. Chem. Soc.* **2012**, *134*, 12338 – 12341.

[24] C. Jarzynski, *Phys. Rev. Lett.* **1997**, *78*, 2690 – 2693.

[25] G. Binnig, C. F. Quate, C. Gerber, *Phys. Rev. Lett.* **1986**, *56*, 930 – 933.

[26] G. Binnig, H. Rohrer, *Surf. Sci.* **1983**, *126*, 236 – 244.

[27] A. Ashkin, J. M. Dziedzic, J. E. Bjorkholm, S. Chu, *Opt. Lett.* **1986**, *11*, 288 – 290.

[28] a) S. B. Smith, Y. J. Cui, C. Bustamante, *Science* **1996**, *271*, 795 – 799; b) K. Visscher, M. J. Schnitzer, S. M. Block, *Nature* **1999**, *400*, 184 – 189.
[29] M. C. Williams, J. R. Wenner, I. Rouzina, V. A. Bloomfield, *Biophys. J.* **2001**, *80*, 1932 – 1939.
[30] a) P. Luchette, N. Abiy, H. Mao, *Sens. Actuators B* **2007**, *128*, 154 – 160; b) H. Mao, P. Luchette, *Sens. Actuators B* **2008**, *129*, 764 – 771.
[31] K. M. Herbert, A. L. La Porta, B. J. Wong, R. A. Mooney, K. C. Neuman, R. Landick, S. M. Block, *Cell* **2006**, *125*, 1083 – 1094.
[32] S. Selvam, D. Koirala, Z. Yu, H. Mao, *J. Am. Chem. Soc.* **2014**, *136*, 13967 – 13970.
[33] a) C. Mao, T. H. LaBean, J. H. Reif, N. C. Seeman, *Nature* **2000**, *407*, 493 – 496; b) P. W. K. Rothemund, *Nature* **2006**, *440*, 297 – 302.
[34] J. Abraham Punnoose, Y. Cui, D. Koirala, P. M. Yangyuoru, C. Ghimire, P. Shrestha, H. Mao, *J. Am. Chem. Soc.* **2014**, *136*, 18062 – 18069.
[35] D. Koirala, Z. Yu, S. Dhakal, H. Mao, *J. Am. Chem. Soc.* **2011**, *133*, 9988 – 9991.
[36] D. Koirala, P. Shrestha, T. Emura, K. Hidaka, S. Mandal, M. Endo, H. Sugiyama, H. Mao, *Angew. Chem. Int. Ed.* **2014**, *53*, 8137 – 8141; *Angew. Chem.* **2014**, *126*, 8275 – 8279.
[37] a) T. M. Frayling, N. J. Timpson, M. N. Weedon, E. Zeggini, R. M. Freathy, C. M. Lindgren, J. R. Perry, K. S. Elliott, H. Lango, N. W. Rayner, B. Shields, L. W. Harries, J. C. Barrett, S. Ellard, C. J. Groves, B. Knight, A. M. Patch, A. R. Ness, S. Ebrahim, D. A. Lawlor, S. M. Ring, Y. Ben-Shlomo, M. R. Jarvelin, U. Sovio, A. J. Bennett, D. Melzer, L. Ferrucci, R. J. Loos, I. Barroso, N. J. Wareham, F. Karpe, K. R. Owen, L. R. Cardon, M. Walker, G. A. Hitman, C. N. Palmer, A. S. Doney, A. D. Morris, G. D. Smith, A. T. Hattersley, M. I. McCarthy, *Science* **2007**, *316*, 889 – 894; b) The Wellcome Trust Case Control Consortium, *Nature* **2007**, *447*, 661 – 678; c) W. E. Evans, M. V. Relling, *Science* **1999**, *286*, 487 – 491.
[38] P. M. Yangyuoru, S. Dhakal, Z. Yu, D. Koirala, S. M. Mwongela, H. Mao, *Anal. Chem.* **2012**, *84*, 5298 – 5303.
[39] A. N. Gupta, A. Vincent, K. Neupane, H. Yu, F. Wang, M. T. Woodside, *Nat. Phys.* **2011**, *7*, 631 – 634.
[40] M. Sassanfar, J. W. Szostak, *Nature* **1993**, *364*, 550 – 553.
[41] T.-H. Nguyen, L. J. Steinbock, H.-J. Butt, M. Helm, R. d. Berger, *J. Am. Chem. Soc.* **2011**, *133*, 2025 – 2027.
[42] D. Koirala, S. Dhakal, B. Ashbridge, Y. Sannohe, R. Rodriguez, H. Sugiyama, S. Balasubramanian, H. Mao, *Nat. Chem.* **2011**, *3*, 782 – 787.
[43] X. Zhang, V. Mar, W. Zhou, L. Harrington, M. O. Robinson, *Genes Dev.* **1999**, *13*, 2388 – 2399.
[44] A. Rajendran, M. Endo, H. Sugiyama, *Curr. Protoc. Nucleic Acid Chem.* **2012**, *48*, 12.19.11 – 12.19.18.
[45] Z. Yu, H. Mao, *Chem. Rec.* **2013**, *13*, 102 – 116.
[46] a) D. Koirala, J. A. Punnoose, P. Shrestha, H. Mao, *Angew. Chem. Int. Ed.* **2014**, *53*, 3470 – 3474; b) S. Mandal, D. Koirala, S. Selvam, H. Mao, *Angew. Chem. Int. Ed.* **2015**, DOI: 10.1002/anie.201502580.

Received: February 1, 2015
Published online on April 27, 2015